

Electronic Supplementary Information

Analysis of ATP and AMP binding to the DNA aptamer and its imidazole-tethered derivatives by surface plasmon resonance

Jing Zhao, Satoshi Katsube, Junpei Yamamoto, Kazuhiko Yamasaki, Makoto Miyagishi and Shigenori Iwai

Experimental Procedures

General methods. Reagents and solvents for the synthesis of the compounds were purchased from Wako Pure Chemical Industries. ^1H - and ^{31}P -NMR spectra were measured on a JEOL JNM-ECS 400 spectrometer, and proton signals were assigned by using COSY spectra. High-resolution mass spectrometry was performed on a Thermo Scientific Exactive spectrometer with electrospray ionization (ESI). The phosphoramidite building block for the incorporation of **1** was prepared according to the literature.²⁸ Oligonucleotides were synthesized, purified by HPLC, and analyzed by ESI-TOF or MALDI-TOF mass spectrometry, at GeneDesign Inc. The amino-tethered oligonucleotides were synthesized using Amino-Modifier C6 dT (Glen Research) at Tsukuba Oligo Service Co., Ltd.

2'-Deoxy-5'-O-(4,4'-dimethoxytrityl)-5-[3-[[[1-(2,4-dinitrophenyl)-1H-imidazol-4-yl]acetyl]amino]-1-propyn-1-yl]uridine (4). In dehydrated pyridine (17 mL), 2'-deoxy-5'-O-(4,4'-dimethoxytrityl)-5-(3-amino-1-propyn-1-yl)uridine (**3**)²⁹ (640 mg, 1.10 mmol) was mixed with the *N*-hydroxysuccinimide ester of 2-[1-(2,4-dinitrophenyl)-1H-imidazol-4-yl]acetic acid³⁰ (1.25 g, 3.21 mmol). After 4 h at 40°C, the solvent was removed by evaporation, and the residue was dissolved in chloroform (200 mL). The solution was washed with water, dried with Na_2SO_4 , and concentrated to dryness on a vacuum rotary evaporator. The product was purified by column chromatography on silica gel, using a stepwise gradient of methanol in chloroform. Compound **4** was obtained as yellowish powder by evaporation. Yield: 817 mg (952 μmol , 89%). ^1H -NMR (400 MHz, dimethyl sulfoxide- d_6 /tetramethylsilane): δ (ppm) 11.57 (s, 1H, CO-NH-CO), 8.88 (d, $J = 2.4$ Hz, 1H, phenyl H3), 8.60 (dd, $J = 9.2, 2.8$ Hz, 1H, phenyl H5), 8.31 (t, $J = 5.2$ Hz, 1H, $\text{CH}_2\text{-NH-CO}$), 7.93 (d, $J = 8.8$ Hz, 1H, imidazole), 7.92 (d, $J = 1.6$ Hz, 1H, imidazole), 7.86 (s, 1H, H6), 7.38–7.14 (m, 9H, DMT), 6.88–6.78 (m, 5H, DMT and phenyl H6), 6.06 (t, $J = 6.4$ Hz, 1H, H1'), 5.26 (d, $J = 4.4$ Hz, 1H, 3'-OH), 4.22 (m, 1H, H3'), 3.90 (d, $J = 5.6$ Hz, 2H, C- $\text{CH}_2\text{-NH}$), 3.91 (m, 1H, H4'), 3.70 (d, $J = 1.2$ Hz, 6H, $-\text{OCH}_3$), 3.40 (s, 2H, CO- $\text{CH}_2\text{-C}$), 3.22 (m, 1H, H5'), 3.05 (dd, $J = 10.4, 2.8$ Hz, 1H,

H5'), 2.19 (m, 2H, H2') (Fig. S2). ESI-HRMS $m/z = 880.25489$ ($[M + Na]^+$ calculated for $C_{44}H_{39}N_7O_{12}Na$: 880.2549).

2'-Deoxy-5'-*O*-(4,4'-dimethoxytrityl)-5-[3-[[[1-(2,4-dinitrophenyl)-1*H*-imidazol-4-yl]acetyl]amino]-1-propyn-1-yl]uridine 3'-[(2-cyanoethyl)-*N,N*-diisopropylphosphoramidite] (5). To a solution of 2'-deoxy-5'-*O*-(4,4'-dimethoxytrityl)-5-[3-[[[1-(2,4-dinitrophenyl)-1*H*-imidazol-4-yl]acetyl]amino]-1-propyn-1-yl]uridine (**4**) (345 mg, 402 μ mol) in tetrahydrofuran (4 mL), *N,N*-diisopropylethylamine (0.28 mL, 1.6 mmol) and (2-cyanoethyl)-*N,N*-diisopropylchlorophosphoramidite (0.18 mL, 0.8 mmol) were added. After 1 h at room temperature, ethyl acetate (90 mL) was added. The solution was washed with 2% aqueous $NaHCO_3$, dried with Na_2SO_4 , and concentrated to dryness on a vacuum rotary evaporator. The product was purified by column chromatography on silica gel, using a stepwise gradient of methanol in chloroform containing 0.1% pyridine. Compound **5** was obtained as reddish powder by evaporation. Yield: 301 mg (284 μ mol, 71%). ^{31}P -NMR (161 MHz, acetone- d_6 /trimethyl phosphate): δ (ppm) 148.95, 148.90. ESI-HRMS $m/z = 1080.36274$ ($[M + Na]^+$ calculated for $C_{53}H_{56}N_9O_{13}NaP$: 1080.3627).

Structure modeling. Structures of the imidazole-tethered aptamers in complex with ATP were modeled, based on the NMR structure of the ABDA-AMP complex (PDB ID: 1aw4)²³, as follows. The coordinates for the modified bases and ATP were generated by Chem 3D (Perkin Elmer). They were fit into the aptamer-AMP complex structure (the first coordinate of PDB ID: 1aw4) by the alignment function in PyMOL, version 1.5 (Schrödinger, LLC). Single bonds in the imidazole-tethered nucleotides were rotated by a PyMOL function, so that the nitrogen atoms of the imidazole and the oxygen atoms of the DNA phosphates could form hydrogen bonds, as judged by N-O distances less than 3.2 Å.

Table S1 Analysis of the oligonucleotides by ESI-TOF or MALDI-TOF mass spectrometry

Aptamer	Calculated mass ^a	Obtained mass ^a
ABDA	8923.02	8923.40 ^b
ABDA1-a	9084.17	9086.08 ^c
ABDA1-b	9084.17	9086.15 ^c
ABDA1-c	9084.17	9086.16 ^c
ABDA1-d	9084.17	9084.67 ^c
ABDA2-a	9070.15	9069.30 ^b
ABDA2-b	9070.15	9069.50 ^b
ABDA2-c	9070.15	9069.50 ^b
ABDA2-d	9070.15	9069.40 ^b

^a [M – H]⁻; ^b ESI-TOF; ^c MALDI-TOF.

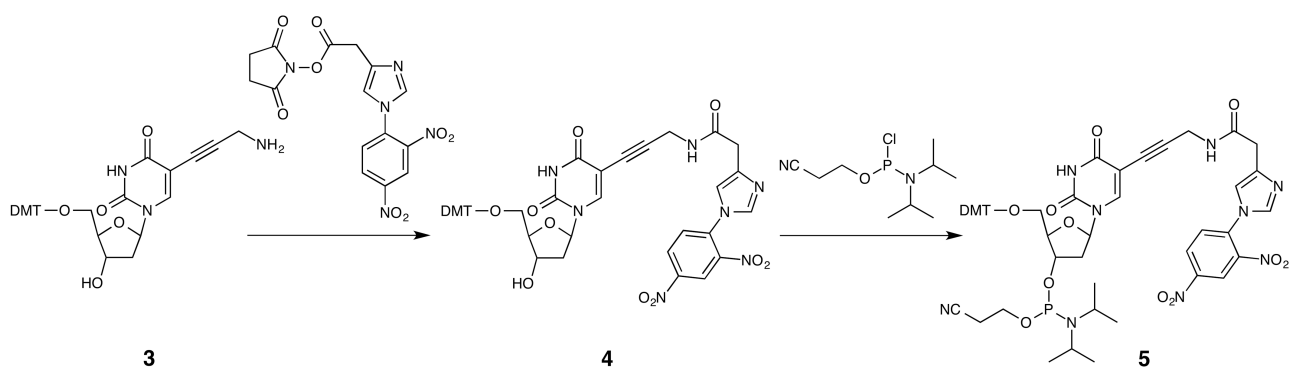


Fig. S1 Synthesis of the building block for the incorporation of **2**. DMT is the abbreviation for 4,4'-dimethoxytrityl.

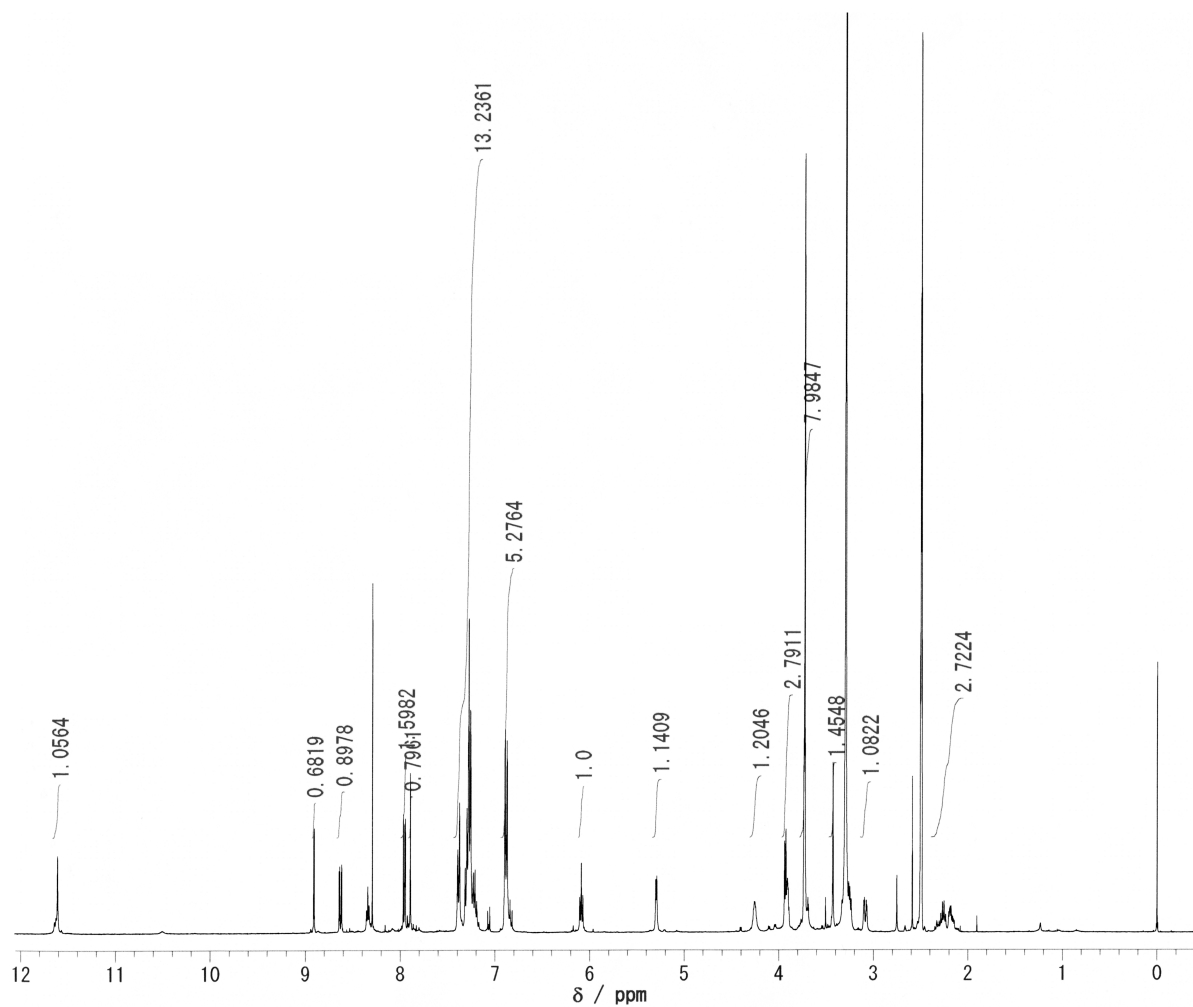


Fig. S2 ^1H NMR spectrum of **4**.

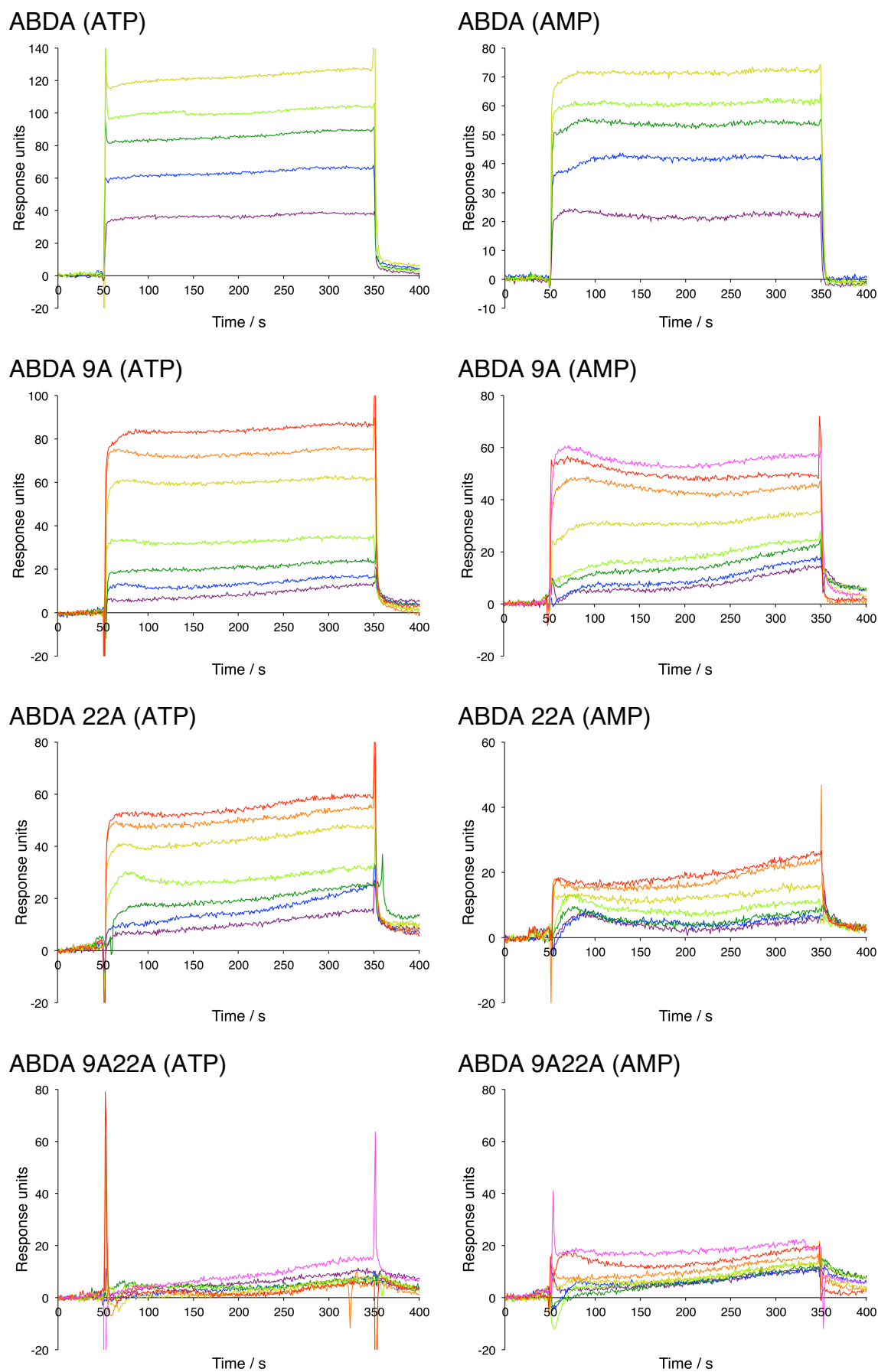


Fig. S3 Sensorgrams of the ATP/AMP binding to the DNA aptamer and its mutants. The concentrations of ATP and AMP were 20, 50, 100, 200, 500, 750, 1,000, and 2,000 μM .

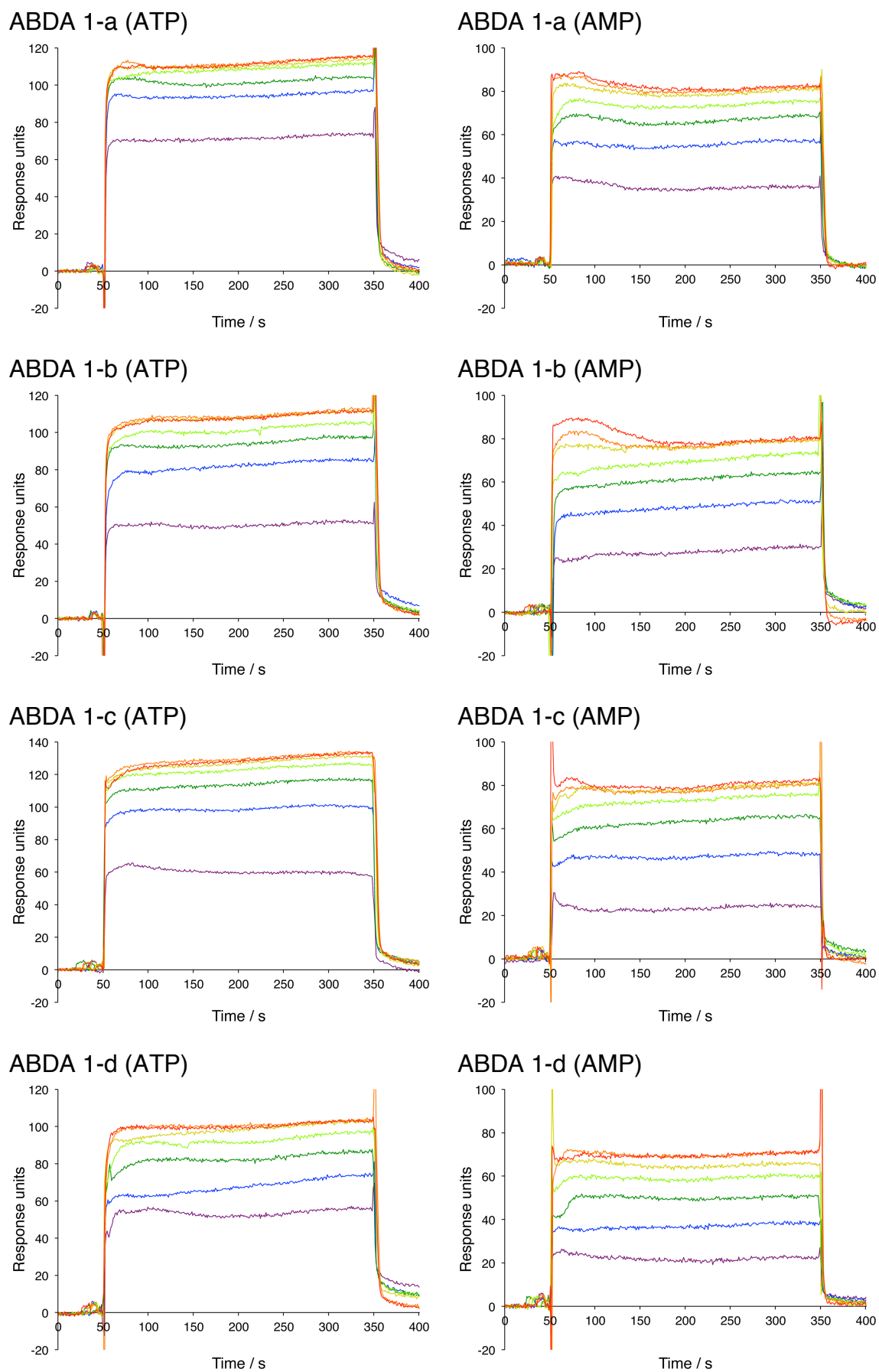
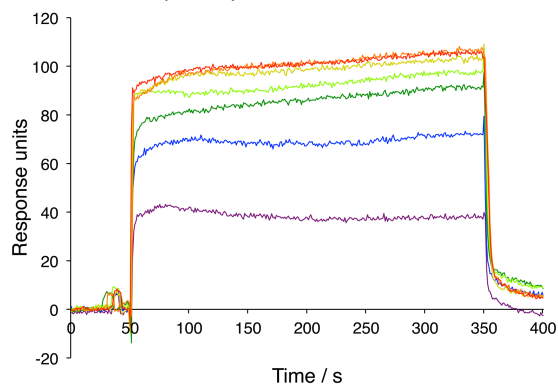
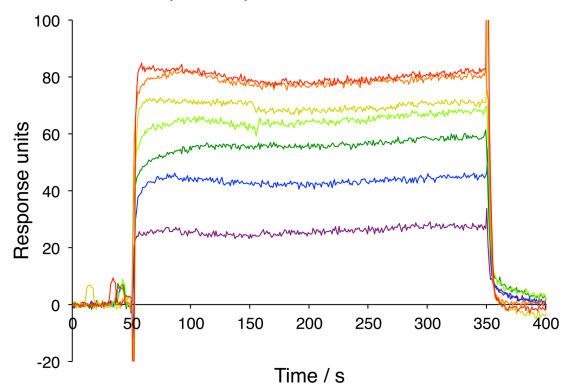


Fig. S4 Sensorgrams of the ATP/AMP binding to the aptamers containing **1**. The concentrations of ATP and AMP were 20, 50, 100, 200, 500, 750, and 1,000 μM .

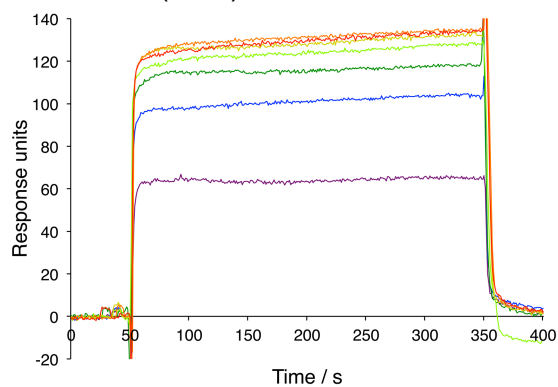
ABDA 2-a (ATP)



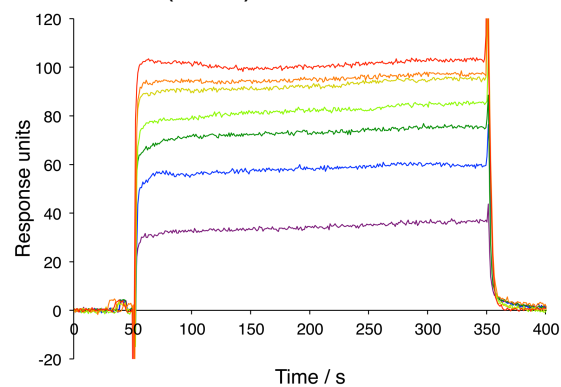
ABDA 2-a (AMP)



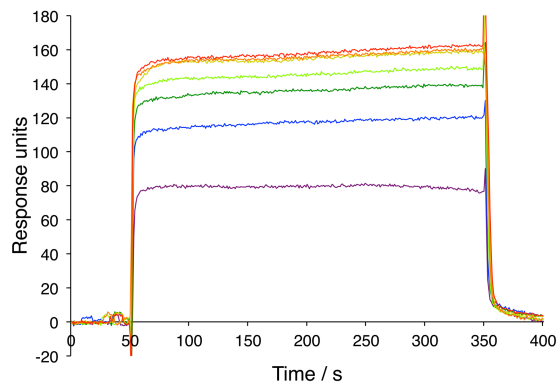
ABDA 2-b (ATP)



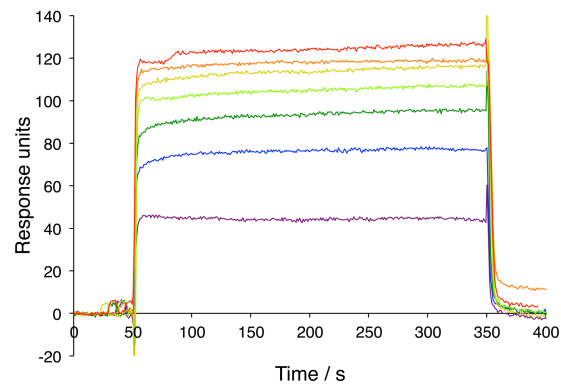
ABDA 2-b (AMP)



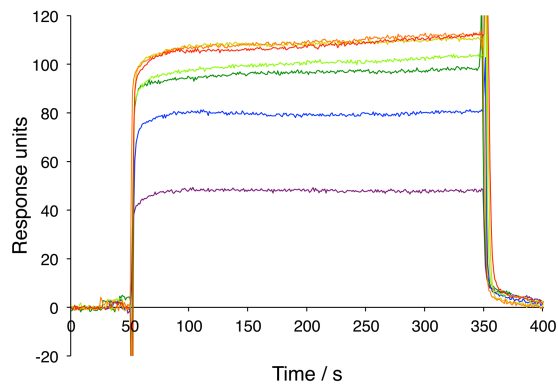
ABDA 2-c (ATP)



ABDA 2-c (AMP)



ABDA 2-d (ATP)



ABDA 2-d (AMP)

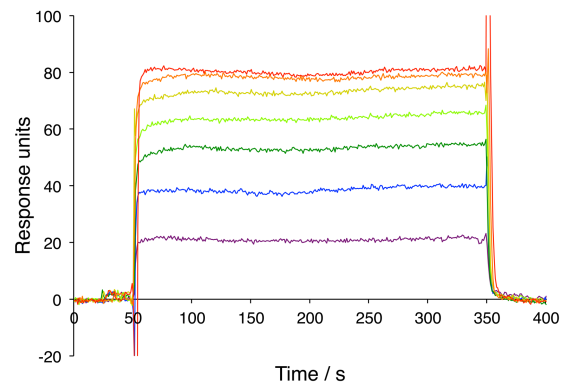


Fig. S5 Sensorgrams of the ATP/AMP binding to the aptamers containing **2**. The concentrations of ATP and AMP were 20, 50, 100, 200, 500, 750, and 1,000 μM .

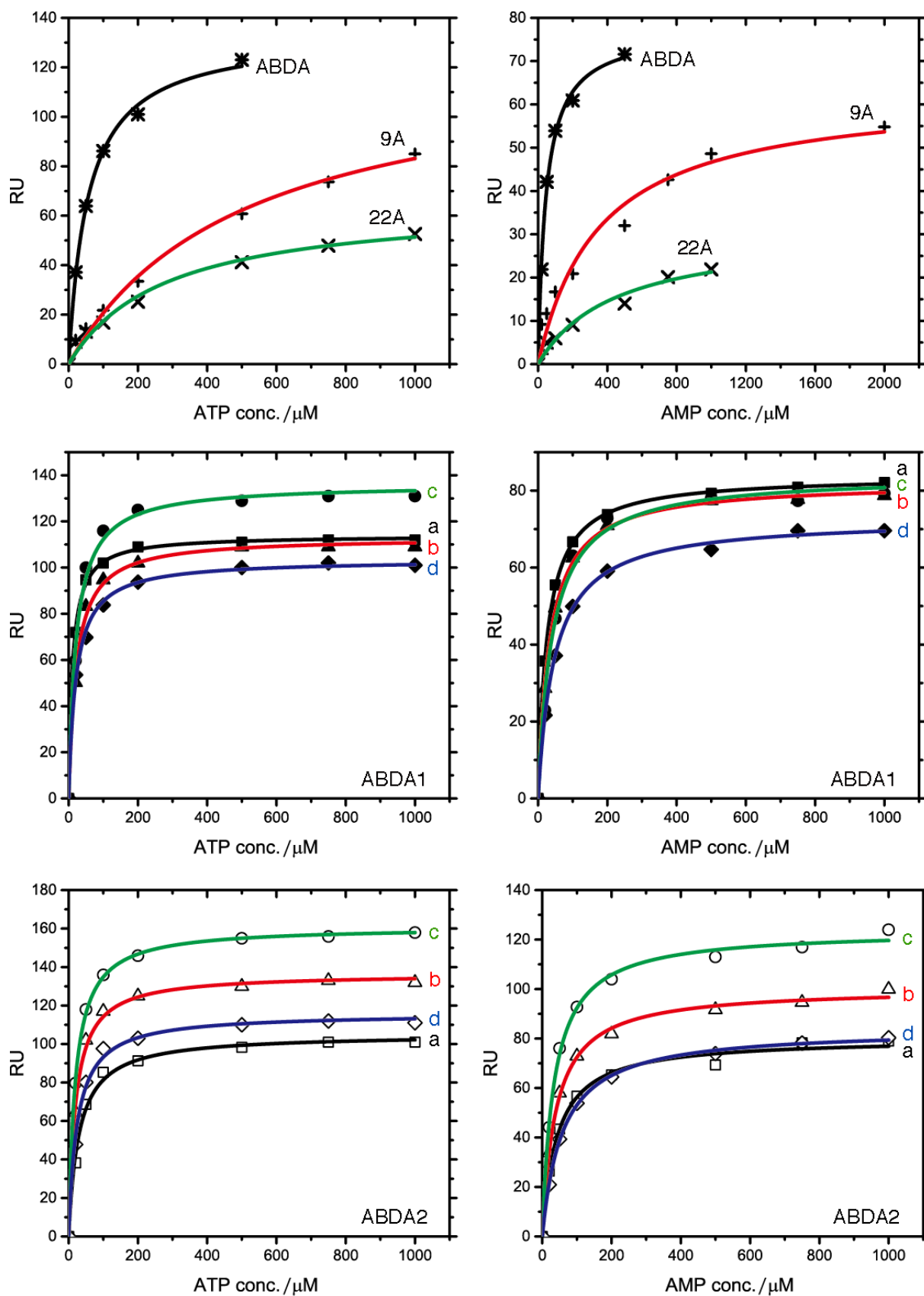
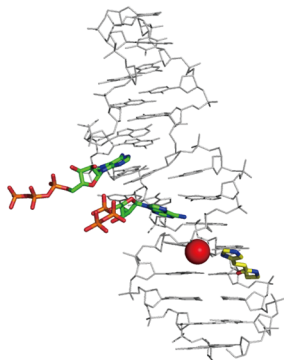
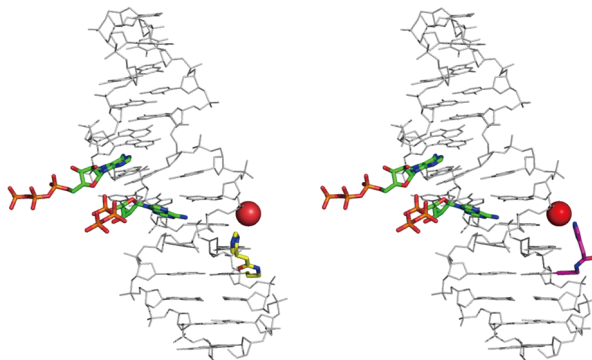


Fig. S6 Curve fitting of the SPR data. The dissociation constants and the stoichiometries obtained from these results are listed in Table 1.

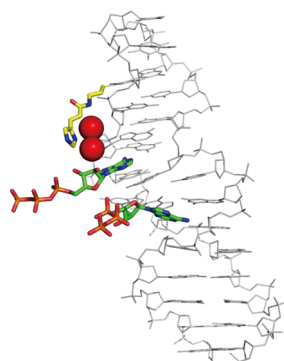
ABDA 1-a



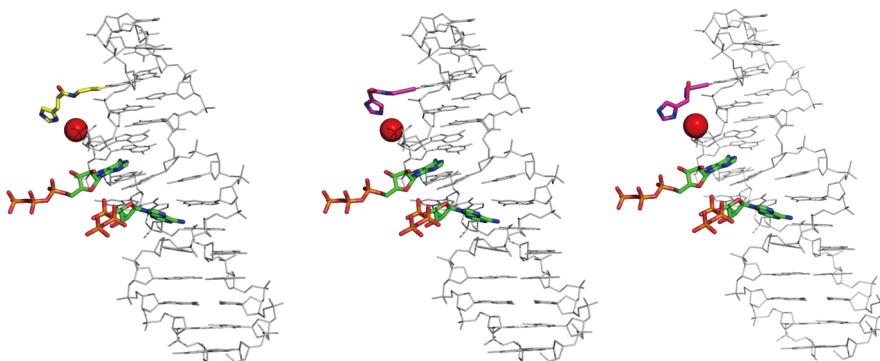
ABDA 2-a



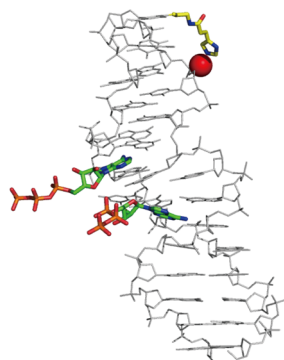
ABDA 1-b



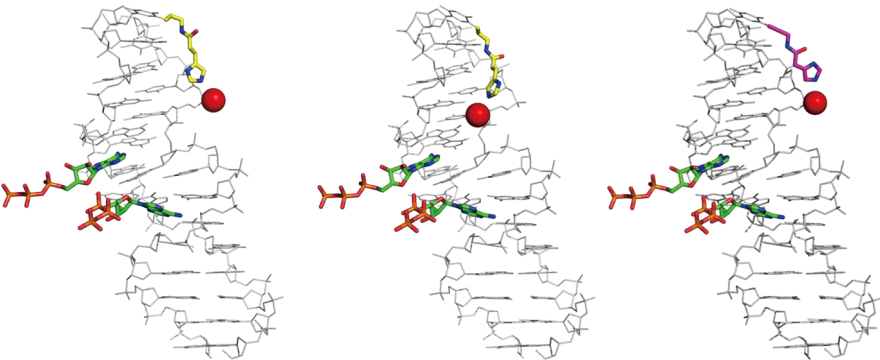
ABDA 2-b



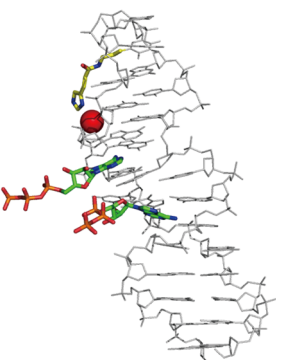
ABDA 1-c



ABDA 2-c



ABDA 1-d



ABDA 2-d

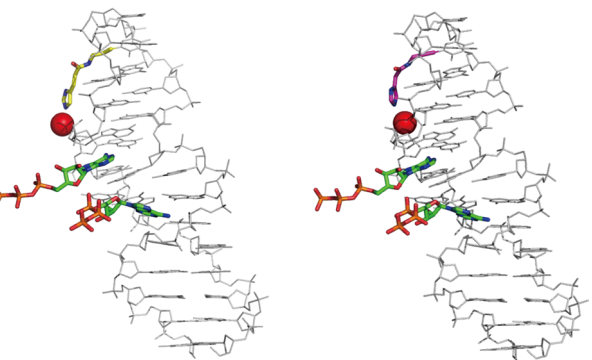


Fig. S7 Modeling of imidazole-tethered aptamer–ATP complexes. The side chains of the modified bases and ATP are shown in stick representations, where the nitrogen, oxygen, and phosphorus atoms are colored blue, red, and orange, respectively, and the carbon atoms in the

side chains of **1** and **2** and ATP are shown in yellow, magenta, and green, respectively. The red spheres are the phosphate oxygen atoms that can interact with the imidazole moiety. The figures were produced by PyMOL, version 1.5.

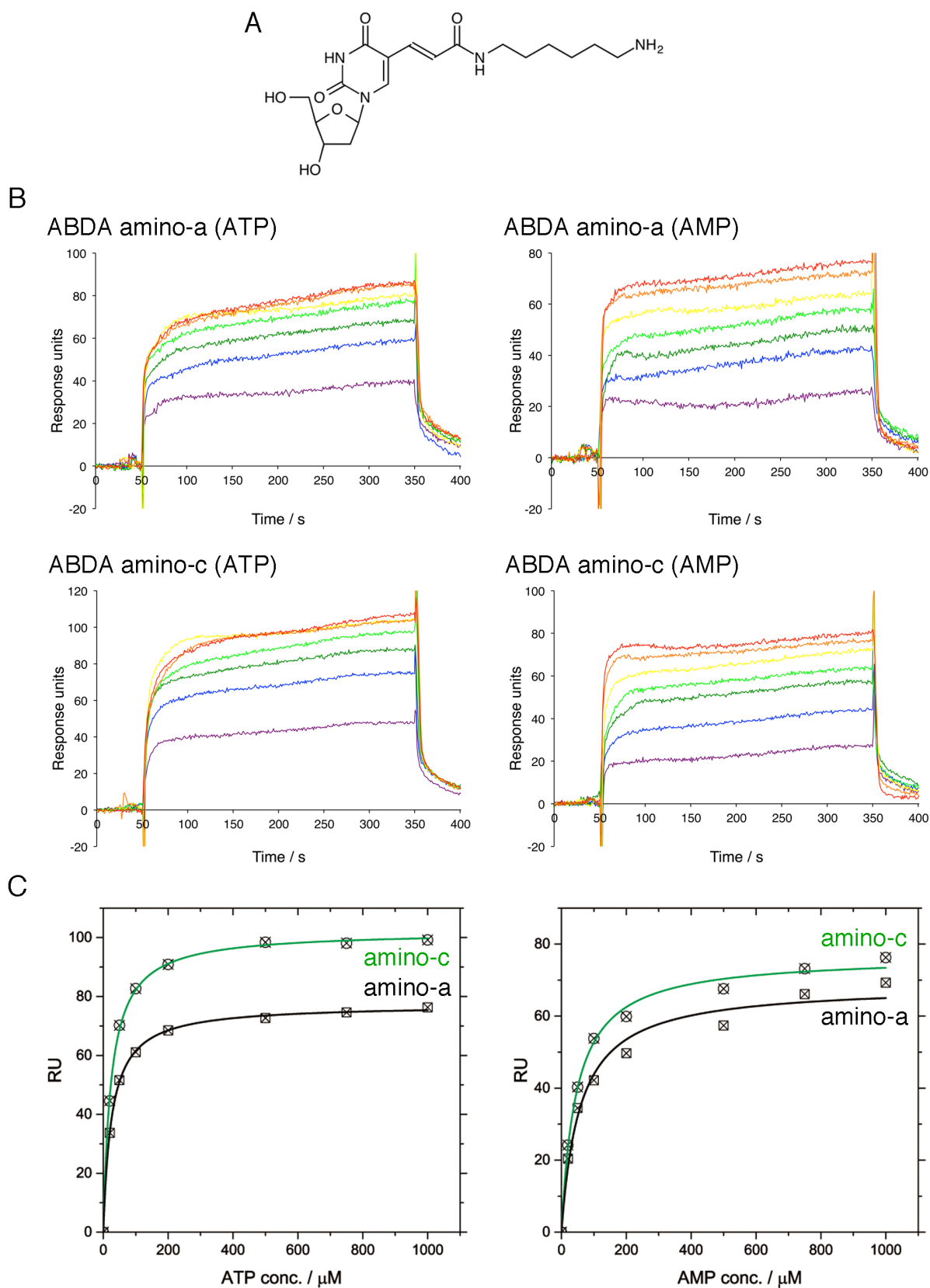


Fig. S8 ATP and AMP binding to the amino-tethered aptamers. (A) Structure of the amino-tethered nucleoside. (B) Sensorgrams of the ATP/AMP binding to the amino-tethered aptamers. The concentrations of ATP and AMP were 20, 50, 100, 200, 500, 750, and 1,000

μM . (C) Curve fitting of the SPR data. The dissociation constants and the stoichiometries obtained from these results are listed in Table 1.